JOURNAL OF VIROLOGY, Feb. 2006, p. 1710–1723 Vol. 80, No. 4
0022-538X/06/$08.00+0 doi:10.1128/JVI.80.4.1710–1723.2006

Phosphorylation of the Varicella-Zoster Virus (VZV) Major Transcriptional Regulatory Protein IE62 by the VZV Open Reading Frame 66 Protein Kinase

Amie J. Eisfeld,[3]† Stephanie E. Turse,[1]† Sara A. Jackson,[4] Edwina C. Lerner,[2] and Paul R. Kinchington[1,2]*

Departments of Ophthalmology[1] and Molecular Genetics and Biochemistry[2] and Graduate Programs in Molecular Virology and Microbiology[3] and Biochemistry and Molecular Genetics,[4] School of Medicine, University of Pittsburgh, Pittsburgh, Pennsylvania 15213

Received 21 July 2005/Accepted 22 November 2005

IE62, the major transcriptional regulatory protein encoded by varicella-zoster virus (VZV), is nuclear at early times of VZV infection but then becomes predominantly cytoplasmic as a result of expression of the protein kinase encoded by open reading frame 66 (ORF66). Cytoplasmic forms of IE62 are required for its inclusion as an abundant VZV virion tegument protein. Here we show that ORF66 directly phosphorylates IE62 at two residues, with phosphorylation at S686 being sufficient to regulate IE62 nuclear import. Phosphotryptic peptide analyses established an ORF66 kinase-mediated phosphorylation of the complete IE62 protein in transfected and VZV-infected cells. Using truncated and point-mutated IE62 peptides, ORF66-directed phosphorylation was mapped to residues S686 and S722, immediately downstream of the IE62 nuclear localization signal. An IE62 protein with an S686A mutation retained efficient nuclear import activity, even in the presence of functional ORF66 protein kinase, but an IE62 protein containing an S686D alteration was imported into the nucleus inefficiently. In contrast, the nuclear import of IE62 carrying an S722A mutation was still modulated by ORF66 expression, and IE62 with an S722D mutation was imported efficiently into the nucleus. An in vitro phosphorylation assay was developed using bacterially expressed IE62-maltose binding protein fusions as substrates for immunopurified ORF66 protein kinase from recombinant baculovirus-infected insect cells. ORF66 kinase phosphorylated the IE62 peptides, with similar specificities for residues S686 and S722. These results indicate that IE62 nuclear import is modulated as a result of direct phosphorylation of IE62 by ORF66 kinase. This represents an interaction that is, so far, unique among the alphaherpesviruses.

Varicella-zoster virus (VZV) is the human herpesvirus that causes chicken pox upon primary infection and herpes zoster following reactivation from a latent state. These diseases are separated by a prolonged period of neuronal latency in which no clinical disease is apparent but a few select viral genes are expressed (15, 25). In a VZV lytic infection, approximately 70 VZV proteins are expressed in a temporally regulated manner (54), most likely in a typical α-β-γ cascade which is transcriptionally regulated in a manner similar to that seen in herpes simplex virus type 1 (HSV-1)-infected cells (19, 20). Several VZV proteins have been implicated in regulating VZV gene expression, based on studies demonstrating their influence on viral promoter-reporter activities in transfection assays. These include the proteins encoded by open reading frames (ORFs) 4, 61, 62, 63, 10, and 29 (reviewed in reference 28).

Of these, the principal transcriptional transactivator of VZV transcription is IE62, encoded by VZV ORF62. This 1,310-amino-acid, heavily phosphorylated protein (30, 31) is expressed with immediate-early (IE) kinetics (13, 30), stimulates transcription from VZV promoters in transfection assays, and enhances the infectivity of VZV DNA (2, 7, 41, 48). It also positively and negatively regulates its own transcription, depending on the cell type (11, 49). While the exact mechanisms underlying IE62-mediated transactivation of viral genes have not been well defined, they are likely similar to those of ICP4 of HSV-1, as IE62 can complement HSV-1 ICP4 mutants and functionally replace ICP4 in the HSV-1 genome (10, 12). ICP4 has been shown to interact with and recruit specific components of the general transcription machinery to viral promoters and to stabilize their formation for transcription initiation (6, 64). VZV IE62 has also been shown to cooperate and interact with both cellular and viral proteins in gene regulation, including USF (52), SP-1 (47), and the viral regulatory proteins from ORFs 4 (58), 47 (4, 45), and 63 (39).

The extensive phosphorylation of IE62 has led to several investigations of its possible interactions with cellular and virally encoded kinases. IE62 is phosphorylated by cellular kinases in the absence of other viral proteins (30, 45). It has two polyserine tracts, one located internally and the other near the C terminus, which are strongly predicted to be sites for casein kinase II. The internal serine tract is conserved in other alphaherpesvirus orthologues and in HSV-1 ICP4 and is a site for phosphorylation by casein kinase II and protein kinase A (62, 63). IE62 is also the target of the VZV Ser/Thr-specific protein kinase encoded by ORF47. ORF47 directly phosphorylates IE62 in vitro and targets sequences resembling those phosphorylated by casein kinase II (26, 45). Whether ORF47 phosphorylates IE62 in vivo and what the consequences of ORF47-directed phosphorylation are on IE62 functions have yet to be defined. While not essential (17), the ORF47 kinase is

* Corresponding author. Mailing address: 1020 Eye & Ear Institute, University of Pittsburgh, 203 Lothrop Street, Pittsburgh, PA 15213. Phone: (412) 647-6319. Fax: (412) 647-5880. E-mail: Kinchingtonp@upmc.edu.

† The first two authors contributed equally to this work.

a tegument protein that is required for efficient virion assembly, efficient growth, and viral pathogenesis in the SCID-hu mouse model (3, 4, 34, 40).

IE62 is also a possible target for the ORF66 protein kinase, as ORF66 expression affects the cellular distribution of IE62. In VZV-infected cells, IE62 expressed at early times of infection enters the cell nucleus by using a single classical arginine/lysine-rich nuclear localization signal (NLS) mapping to amino acids 677 to 685 (33). However, at late stages of infection, IE62 accumulates predominantly in the cytoplasm (30, 33). This activity is mediated by ORF66 protein kinase, as IE62 remains nuclear in cells infected by a recombinant VZV that does not express ORF66. Furthermore, progeny viruses from VZV-infected cells not expressing ORF66 do not incorporate IE62 as an abundant virion protein (29). Thus, IE62 cytoplasmic accumulation and/or its targeting by ORF66 is required for virion inclusion of IE62 as an abundant tegument protein (29, 30). Cotransfection studies indicated that the ORF66 kinase is sufficient to induce the cytoplasmic accumulation of IE62 independent of other VZV proteins (30, 33). Since VZV recombinants lacking ORF66 expression demonstrate considerable impairment for growth in human T lymphocytes (40, 55, 57), the ORF66-induced effects on IE62 cellular distribution and inclusion in the virion structure may be important in the pathogenesis of VZV. Furthermore, a single report has suggested that ORF66 is expressed during VZV latency in human ganglia (9). While not yet confirmed, this could mechanistically explain reports of a predominantly cytoplasmic distribution of IE62 in latently infected neurons (15, 38). The cytoplasmic accumulation of IE62 induced by ORF66 requires the integrity of the ORF66 kinase activity, suggesting that phosphorylation is a necessary step for affecting IE62 cellular redistribution. In agreement with this, small IE62 peptides responsive to ORF66-mediated cytoplasmic redistribution were found to be preferentially phosphorylated in cells coexpressing the ORF66 kinase (30).

It has not been determined whether IE62 phosphorylation occurs as a result of ORF66 activation of cellular pathways or if IE62 represents a direct target for the ORF66 protein kinase. In this work, we precisely map ORF66-mediated phosphorylation of IE62, show that ORF66 directly phosphorylates the IE62 protein in vitro, and demonstrate that one of the phosphorylation events leads to IE62 cytoplasmic accumulation. Thus, IE62 represents a new viral target for the US3 kinase group.

MATERIALS AND METHODS

Cells and virus. VZV was grown on the human melanoma cell line MeWo (obtained from C. Grose, University of Iowa), as detailed previously (29). 293T cells (ATCC) were maintained in Dulbecco's modified Eagle's medium supplemented with 5% fetal bovine serum, 100 U penicillin, 100 μg/ml streptomycin, and 0.25 μg/ml amphotericin B. Cosmid-derived recombinant VZV ROka, ROka47S (not expressing ORF47), and ROka66S (not expressing ORF66) have been detailed previously (17, 18) and were a kind gift from J. I. Cohen (Laboratory of Clinical Investigation, NIH). VZV stocks were prepared and stored as previously described (27, 31). For transient expression studies, MeWo cells at 70% confluence were transfected using Lipofectamine with the Plus reagent (Invitrogen Corp., Carlsbad, CA), as detailed previously (30). 293T cells were transfected at 50 to 70% confluence, using a modified calcium phosphate coprecipitation method, with 30 μg total plasmid DNA transfected in 1 ml total of HEPES-buffered saline and divided between two 60-mm dishes containing 5 ml of medium/dish. Cells were exposed to the precipitate in the medium overnight, followed by medium replacement. In all comparative transfection studies, the total amount of the human cytomegalovirus (HCMV) major IE promoter used to drive gene expression was equalized by adding a corresponding amount of empty vector. Baculoviruses were grown in SF9 cells (Invitrogen Corp.) at 28°C in Grace's insect medium supplemented with 5% fetal bovine serum and antibiotics, as detailed by the supplier.

Antibodies and immunological methods. Polyclonal rabbit antibodies that recognize IE62 and the ORF66 protein kinase have been described previously (9, 29, 30). Antibodies to the nine-amino-acid epitope YPYDVPDYA of the influenza virus hemagglutinin (HA) protein were initially obtained from Santa Cruz Biotechnologies, Inc. (Santa Cruz, CA) and were later derived by using a monoclonal antibody (48EC) developed against the synthetic peptide by the Hybridoma Core Facility of the University of Pittsburgh Department of Ophthalmology. Immunofluorescence, immunoblotting, and immunoprecipitation were carried out as detailed previously (30), except that bound antibodies in immunoblotting studies were detected using secondary goat anti-rabbit or goat anti-mouse antibodies coupled to horseradish peroxidase (ICN/Cappel, Aurora, OH), followed by detection with West Dura chemiluminescent substrate (Pierce, Inc., Rockford, IL). Quantitation of protein band signals was achieved either with a Bio-Rad GS525 phosphorimager or by densitometry of autoradiographs exposed to be in the linear range of the film.

Plasmids and DNAs for transfection. The following constructs have been detailed previously (30, 33): pG310 expression vector, pGK2-HA expression vector, pKCMV62, pKCMV47, pGK2-HA47, pKCMV66, pGK2-HA66, and pGK2-HA66-K122A. Briefly, the pG310 and pGK2-HA vectors contain the complete HCMV IE promoter, followed by EcoRI and BamHI sites for gene insertion, and a polyadenylation signal derived from the HCMV IE1 gene. pGK2-HA is similar to pG310 but additionally contains an initiating methionine followed by the sequence encoding the HA epitope (YPYDVPDYA) and then the same cloning sites. Plasmids pKCMV66 and pKCMV66-K122A express wild-type ORF66 and a point-inactivated kinase-dead ORF66 altered at K122, the residue suspected to be required for binding ATP, respectively; pGK2-HA66 and pGK2-HA66-K122A express the same proteins as N-terminally HA-tagged forms. Plasmid pGK2-HA47 expresses HA-tagged ORF47, and pKCMV62 expresses the untagged full-length IE62 protein.

The following new IE62 peptide-expressing constructs were developed, using PCR amplification with the proof-reading polymerase Expand (Roche Biochemicals, Inc.): pGK2-HA846, pGK2-HA825, pGK2-HA819, pGK2-HA821, pGK2-HA823, pGK2-HA810, pGK2-HA828, and pGK2-HA811. The primers used are listed in Table 1. pGK2-HA846 was generated by EcoRI linker addition (New England Biolabs, Inc., Beverly, MA) to an EcoRV-BstXI DNA fragment of IE62 (positions 122,010 to 123,232 [residues 414 to 823 of IE62] with respect to the VZV Dumas sequence), followed by digestion with EcoRI and BamHI (the BamHI site is at position 122,962 [residue 735 of IE62]). Cloning this fragment into the pGK2-HA vector resulted in the expression of IE62 residues 414 to 735 in frame with the HA epitope tag. Additional constructs from pGK846 were derived by replacement of a DNA fragment, defined by a unique KpnI site at position 122,475 (residue 571 of IE62) and the unique BamHI site, with either double-stranded complementary oligonucleotide primers or KpnI- and BamHI-digested PCR amplification products. Accordingly, pGK2-HA810 expressed residues 414 to 687; pGK2-HA828 expressed residues 414 to 571 fused in frame to residues 673 to 735; pGK2-HA825 expressed residues 414 to 571 fused in frame to residues 656 to 735; pGK2-HA811 expressed residues 414 to 571 fused to residues 677 to 735; pGK2-HA819 expressed residues 414 to 571 fused to the nuclear localization signal of IE62, defined by residues 677 to 686 (33); pGK2-HA821 expressed residues 414 to 571 fused to residues 386 to 394 of the VZV ORF61 protein, corresponding to the ORF61 nuclear localization signal (ARGAKRRL) (59); and pGK2-HA823 expressed residues 414 to 571 fused in frame to the nuclear localization signal for simian virus 40 (SV40) (PPK KKRKV) (53). A second set of constructs was derived from the plasmid pGK2-HA846, containing point mutations resulting in the substitution of alanines for specific serine/threonine residues between amino acids 680 and 735 of IE62 (Table 1). Mutations were carried out by site-specific mutagenesis using the Gene Editor system (Clontech Corp., Palo Alto, CA). To derive full-length IE62 proteins with selected amino acid changes, the KpnI-BamHI fragment from pKCMV62 was replaced with the corresponding KpnI-BamHI fragments derived from site-specifically altered pGK2-HA846 derivatives, resulting in plasmids pKCMV62-S686A, pKCMV62-S686D, pKCMV62-S722A, and pKCMV62-S722D. All DNAs were prepared for transfection using QIAGEN columns.

To derive maltose binding protein (MBP)-IE62 fusions, the portion of the IE62 gene defined by the KpnI-BamHI sites in IE62 (encoding residues 571 to 735) was inserted into the KpnI and BamHI sites of pMalcR1 (New England Biolabs), followed by in-frame alignment of the maltose binding protein and the IE62 ORF by digestion with KpnI, treatment with T4 DNA polymerase and

TABLE 1. Primers used for the derivation of constructs

Vector	Sequence (5′–3′)	Primer type[a]
pGK2-HA810	GGCGGGTACCGCCGTTACGG	K
	GCGGATCCGACTTGCGCTTGCGC	B
pGK2HA828	GGCGGTACCCCACCGGATGATCGT	K
	GCGGATCCACCACAGGGCCCGAGG	B
PGK2-HA825	GCGGGGTACCCAGGCTCCCGACC	K
	GCGGATCCACCACAGGGCCCGAGG	B
PGK2-HA811	GCGGGGTACCCGTTTACGAACTCCG	K
	GCGGATCCACCACAGGGCCCGAGG	B
PGK2-HA819	CCGTTTACGAACTCCGCGCAAGCGCAAG	S
	GATCCTTGCGCTTGCGAGTTCGTAAAC GGGTAC	AS
PGK2-HA821	CGCAAGGGGTGCTAAGCGCCGGTTG	S
	GATCCAACCGGCGCTTAGCACCCCTTG CGGTAC	AS
PGK2-HA823	CCCGCCGAAGAAGAAGCGCAAGGTG	S
	GATCCACCTTGCGCTTCTTCTTCGGCG GGGTAC	AS
M726/28/29	GAGCCCGTGGCCATCGCCGCGGGCCCT GTG	
M715/22	ATGTGGTTGCCAAGGCCAAGAGGCGGG TAGCCGAGCCCG	
M715	ATGTGGTTGCCAAGGCC	
M722	AGGCGGGTAGCCGAGCCCG	
M686	CAAGCGCAAGGCCCAGCCAG	
M91/93/701	CCAGTCGAGGGCAGAGGCCTCCTC and GATTAGGGAGGCACCCGTCGCG	
MS686D	CGCAAGCGCAAGGACCAGCCAGTCGAGA	
M722D	AAGAGGCGGGTCGACGAGCCCGTGA	

[a] K, PCR N-terminal primer with KpnI site; B, PCR C-terminal primer with BamHI site; S, sense primer (coding); AS, antisense primer. For mutating primers (M), the altered residues are underlined.

deoxynucleoside triphosphates, and subsequent religation. For the expression of forms of MBP-IE62 fusion proteins containing mutations, the corresponding NotI-BamHI fragments (encoding residues 602 to 735) were switched between the pGK2-HA846-based constructs and the maltose binding protein–IE62 571-735 derivative.

Phosphorylation analyses. ^{32}P-labeled IE62 peptides for phosphotryptic peptide analysis were generated from transfected cells incubated in growth medium containing 5% serum, 1/20 the normal amount of phosphate, and [^{32}P]orthophosphate at 500 μCi/ml for 8 to 12 h, initiating at 16 h posttransfection. Immunoprecipitations were carried out as detailed previously (30), using a modified buffer (50 mM HEPES-KOH [pH 7.4], 150 mM NaCl, 1% Nonidet P-40, 0.5% sodium deoxycholate, 1 mM EDTA, and 1 mM dithiothreitol) containing a protease inhibitor cocktail (Complete Mini EDTA-free; Roche Applied Sciences, Indianapolis, IN) and the phosphatase inhibitors 2 mM $NaVO_4$ and 25 mM NaF to solubilize proteins. Labeled proteins were separated by sodium dodecyl sulfate-polyacrylamide gel electrophoresis (SDS-PAGE) and identified by autoradiography.

Two-dimensional phosphopeptide analyses were carried out as detailed previously (5). Briefly, immunoprecipitated, SDS-PAGE-separated, ^{32}P-labeled IE62 proteins were transferred to Immobilon-P membranes and identified by autoradiography, and the membrane fragments containing the labeled proteins were excised. Membranes were washed sequentially in 0.5% polyvinylpyrrolidone in 100 mM acetic acid for 30 min, water for 10 min, and then 50 mM ammonium bicarbonate for 10 min. IE62 peptides were released by two sequential digestions in 200 μl of 5 mM ammonium bicarbonate containing 10 to 20 μg tosylsulfonyl phenylalanyl chloromethyl ketone-treated trypsin at 37°C for 24 h and then again for 4 h. Released peptides were concentrated by freeze-drying and then spotted onto silica thin-layer chromatography (TLC) sheets in a 1- to 3-mm spot. The resolution of peptides in the first dimension was done by electrophoresis in a buffer of formic acid, glacial acetic acid, and water at a ratio of 25:78:897 and at pH 1.9. TLC sheets were dried, and peptides were subsequently resolved in the second dimension by ascending chromatography in phosphochromatography buffer (15:10:3:12 ratio of *n*-butanol to pyridine to glacial acetic acid to water). ^{32}P-labeled IE62 peptides were then identified by autoradiography, using Kodak Biomax imaging screens and film.

Baculovirus construction and in vitro phosphorylation analyses. Baculoviruses expressing the HA-tagged ORF66 protein kinase were derived using the BaculoGold system (BD Pharmingen, San Diego, CA). The complete HA-tagged ORF66 gene with the HCMV IE1 polyadenylation signal was excised from pGK2-HA66 and cloned into the baculovirus transfer vector pVL1392 (BD Pharmingen). Following cotransfection with BaculoGold DNA into SF9 cells, progeny virus was isolated and amplified. Expression of the HA-ORF66 protein kinase in infected SF9 cells was verified by immunoblot analysis with HA-specific antibodies. The baculovirus-generated ORF66 protein of 55 kDa was the same size as the HA-ORF66 protein present in extracts of pGK2-HA66-transfected 293T cells. For in vitro kinase activity and in vitro phosphorylation, immunoprecipitates were prepared from SF9 cells infected with either a baculovirus expressing HA-tagged ORF66 (Bac-HA66) or a control baculovirus expressing glutathione *S*-transferase (Bac-GST). Proteins were solubilized using radioimmunoprecipitation (RIPA) buffer (20 mM Tris-HCl [pH 7.4], 50 mM KCl, 1% NP-40, and 0.5% deoxycholate) plus a protease inhibitor cocktail and phosphatase inhibitors (as detailed above), and ORF66 was precipitated using monoclonal antibodies specific for the HA epitope tag. An unrelated, nonspecific control monoclonal antibody was used for control immunoprecipitates where indicated (a gift of N. Sundar-Raj, Department of Ophthalmology, University of Pittsburgh). In some studies, a competing HA peptide or a nonspecific peptide derived from the VZV ORF29 C-terminal domain (32) was added to the SF9 cell extracts at a final concentration of 0.2 mg/ml prior to the addition of monoclonal antibody. After being extensively washed with RIPA buffer, beads were washed in a kinase buffer (20 mM HEPES [pH 7.5], 50 mM KCl, 0.1 mM EDTA, and 10 mM $MgCl_2$ or 50 mM $MnCl_2$, as indicated in the text) and then incubated in 50 μl kinase buffer containing 10 μg/ml heparin and 5 μCi of [γ-^{32}P]ATP (6,000 Ci/mmol) at 35°C for 30 min. Reactions were halted by the addition of SDS sample buffer, proteins were separated by SDS-PAGE, and phosphorylated bands were detected by autoradiography.

MBP-IE62 protein substrates for in vitro phosphorylation reactions were expressed in *Escherichia coli* and purified as detailed previously (27) and as recommended by the manufacturer (New England Biolabs, Inc.), except that the induction of MBP fusion proteins was carried out at 30°C for 3 h and the pellets were sonicated four times for 30 seconds each at 4°C to release fusion proteins. In vitro kinase assays were performed using approximately 5 μg of MBP fusion substrates with an equally divided HA-ORF66 immunoprecipitate so that each reaction received an identical amount of kinase.

RESULTS

Phosphopeptide analysis of IE62 expressed with and without VZV protein kinases. Previously, we showed that the dramatic redistribution of the VZV IE62 nuclear localizing protein to the cytoplasm was dependent on the integrity of the VZV-encoded ORF66 kinase activity (30, 33). However, it was difficult to demonstrate specific ORF66-mediated IE62 phosphorylation within the full-length IE62 protein because the extensive phosphorylation of IE62 protein by cellular kinases masked any ORF66-mediated events (30, 31, 45). Increased phosphorylation induced by ORF66 could only be demonstrated for IE62 peptides missing large regions that are strong targets for cellular protein kinases (30). While these data implied that the ORF66 kinase influenced the phosphorylation of IE62, we considered it important to demonstrate differential phosphorylation induced by ORF66 in the context of the complete IE62 protein. We also reasoned that similar approaches might reveal whether the ORF47 kinase can mediate novel phosphorylation of IE62 in vivo, as suggested by in vitro (26, 45) studies.

To characterize the complexity of IE62 phosphorylation, we used a tryptic phosphopeptide mapping procedure, as detailed previously (5). Phosphorylation of IE62 was first examined in the presence of the VZV protein kinases (at a 1:1 ratio) in cotransfected 293T cells. Following metabolic labeling in medium containing [^{32}P]orthophosphate for 8 h, IE62 was immunoprecipitated, separated by SDS-PAGE, and transferred to Immobilon P membranes. The amounts of ^{32}P label incorporated into IE62 proteins obtained under all conditions were similar, and the mobility of [^{32}P]IE62 in SDS-PAGE was not detectably different under each condition (data not shown).

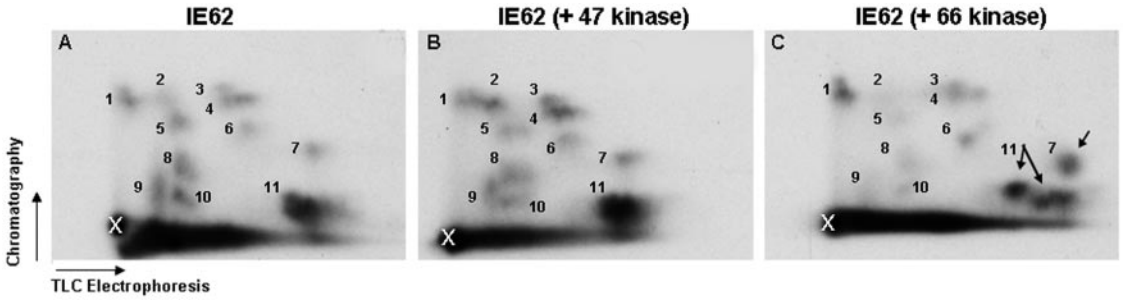

FIG. 1. Full-length IE62 is differentially phosphorylated in the presence of ORF66 kinase. IE62 was expressed in the absence (A) or presence of ORF47 (B) or ORF66 kinase (C) in transfected 293T cells, metabolically labeled with [^{32}P]orthophosphate, immunoprecipitated, and subjected to tryptic phosphopeptide mapping as described in Materials and Methods. The X in the lower left corner of each map indicates the origin of spotting of the peptides. The horizontal axes represent electrophoresis of the peptides on TLC plates, and the vertical axes represent the chromatography step. Phosphopeptide spots are labeled with numbers to facilitate reference from panel to panel, and arrows in panel C indicate the differences in spots generated by coexpression of IE62 with the ORF66 kinase that are discussed in the text.

Tryptic phosphopeptides released from membrane-immobilized IE62 proteins were extracted, separated in two dimensions, and detected by autoradiography as detailed in Materials and Methods. Since the technique showed some variability in separate runs, all comparative studies were carried out in parallel and under identical conditions. Autoradiographs revealed complex tryptic phosphopeptide maps for IE62, even in the absence of any VZV protein kinases, substantiating IE62 as a target for cellular kinases. At least 11 peptides could be readily identified (Fig. 1A). The peptide maps for IE62 expressed alone and IE62 expressed in the presence of ORF47 were very similar, with most peptides migrating to similar positions (Fig. 1B). Only very minor differences were apparent, suggesting that ORF47 did not greatly affect the phosphorylation state of IE62 in vivo. In contrast, the peptide map for IE62 expressed in the presence of ORF66 showed numerous changes, both in the relative abundance of several phosphopeptides (spots 5, 8, 9, and 10 were reduced) and in the appearance and/or movement of at least two novel phosphopeptide spots (Fig. 1C, arrows). In particular, peptide 11 in the map for IE62 expressed in the absence of any kinase was altered in the map for ORF66 coexpressed with IE62 to at least two, and possibly three, peptides (indicated by arrows), and peptide 7 migrated further in the electrophoresis direction from the origin. We concluded that ORF66 induces a differential phosphorylation state of the complete IE62 protein.

Similar approaches were used to address IE62 phosphorylation in the context of VZV-infected MeWo cells, using recombinant VZV strains that do not express kinases (Fig. 2). Following equivalent infections with VZV-ROka, ROka47S (not expressing ORF47), and ROka66S (not expressing ORF66) at a ratio of 1 infected cell to 20 uninfected cells and a 12-h metabolic labeling period with [^{32}P]orthophosphate initiating at 18 h postinfection, IE62 was immunoprecipitated and analyzed by tryptic phosphopeptide mapping. The phosphopeptide map for ROka66S IE62 (produced in the absence of ORF66 expression) exhibited a general reduction in many of the IE62 phosphopeptides compared to that for ROka IE62, despite equal loading of counts onto the TLC plates (Fig. 2C). Furthermore, we observed one IE62 peptide spot (labeled 7b) that was abundant in both ROka and ROka47S IE62 which demonstrated a considerably reduced signal in ROka66S IE62 (Fig. 2C, arrow). These observations indicated that ORF66 induced novel phosphorylation events on the whole IE62 protein in the context of VZV infection. A comparison of the ROka and ROka47S IE62 protein maps revealed very minor differences (Fig. 2A and B), indicating that ORF47 does not

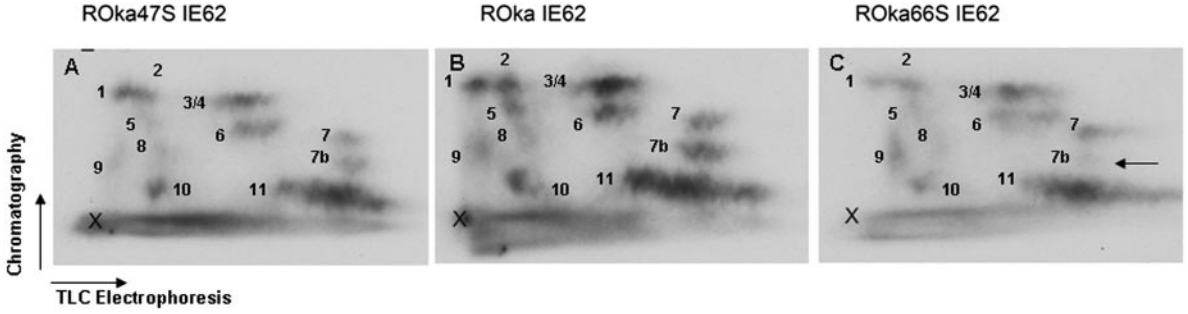

FIG. 2. IE62 is differentially phosphorylated in the presence of ORF66 in the context of VZV infection. Tryptic phosphopeptide maps were generated from IE62 obtained from ^{32}P-labeled VZV-infected cells by immunoprecipitation, as described in Materials and Methods and in the legend to Fig. 1. IE62 was derived from MeWo cells infected with VZV ROka47S (not expressing ORF47) (A), VZV ROka (B), and VZV ROka66S (not expressing ORF66) (C). The X in the lower left corner of each map indicates the origin of spotting of the peptides. The arrow in panel C indicates a phosphopeptide which is reduced in ROka66S IE62.

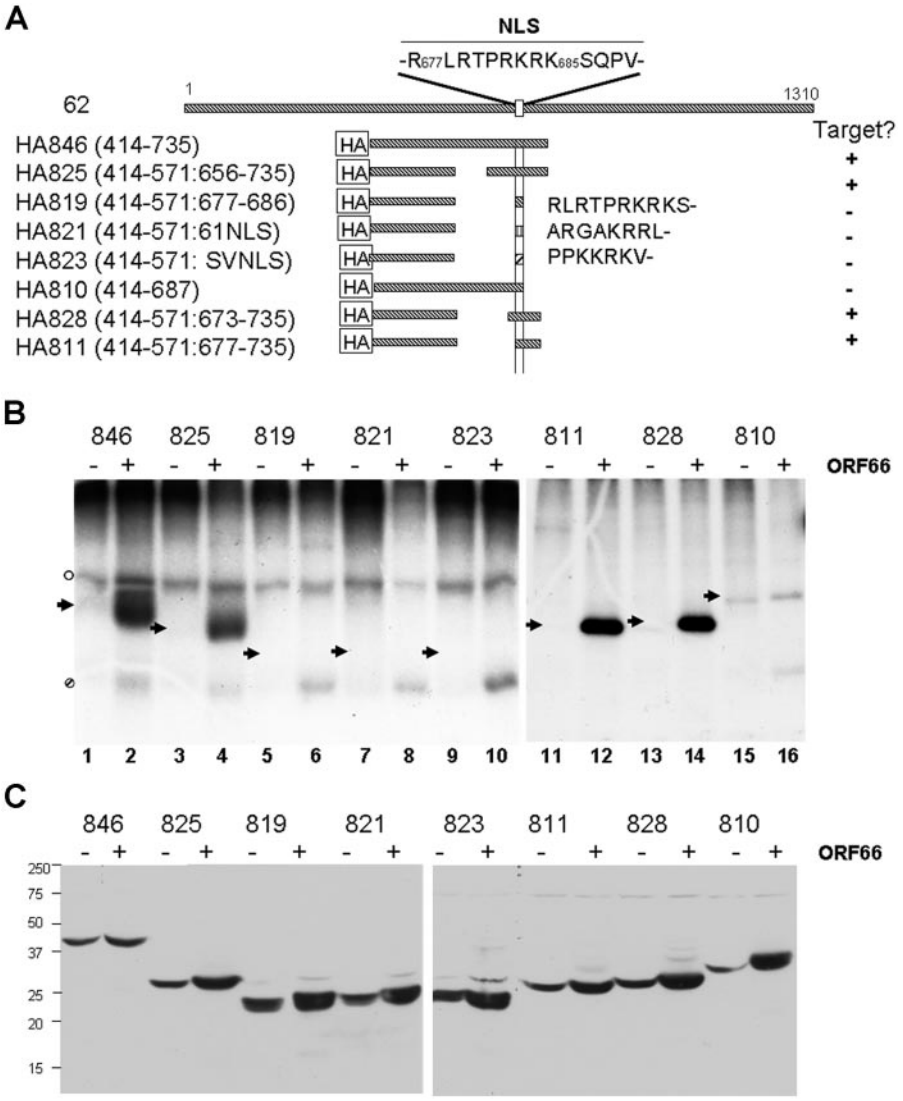

FIG. 3. Mapping of VZV ORF66 kinase-induced phosphorylation of IE62 peptides. (A) Schematic representation of IE62 peptides used for this work. The top line represents the full-length IE62 protein and the relative position of its NLS (33), which is shown above the line in single-letter code, with key residues numbered according to their positions in IE62. Lines beneath full-length IE62 represent the peptides expressed relative to the complete IE62 protein. The precise residues expressed from each construct are indicated to the left of each representation, and for constructs expressing NLSs of other proteins in conjunction with a 414-571 IE62 peptide, the NLS sequences are indicated in single-letter code to the right of the representations. ORF66-specific phosphorylation of the peptide (Target?) is indicated to the right. (B) SDS-PAGE-separated, immunoprecipitated, ^{32}P-labeled IE62 peptides expressed from the constructs shown in panel A, either in the presence (+) or in the absence (−) of ORF66 kinase. Arrowheads indicate the expected sizes of the expressed IE62 peptides for reference in the text. Nonspecific phosphopeptides detected in both the presence and absence of ORF66 in some studies are indicated by an open circle, and an unidentified protein coprecipitating with the IE62 peptide expressed in ORF66 kinase-positive cells is identified by a hatched circle. Lane numbers are indicated at the bottom of the radiograph. (C) Immunoblot detection of the same respective peptides expressed in 293T cell extracts obtained from a similar transfection, showing the relative levels of peptides expressed in the absence (−) or presence (+) of a 1:1 ratio of the ORF66 protein kinase. The peptides were detected with an HA-specific antibody. Molecular masses of marker proteins and their relative mobilities are shown to the left of the blots.

grossly affect most of the phosphorylation events that occur on IE62 in the context of VZV infection in MeWo cells.

Fine mapping of ORF66-mediated phosphorylation of IE62. Because novel phosphorylation of IE62 induced by ORF66 has not been reported for corresponding orthologous proteins in other alphaherpesviruses, we took approaches to map the phosphorylation sites in detail. We were unable to unambiguously identify the novel ORF66-induced peptides seen in the ORF66-IE62 cotransfection peptide map (Fig. 1C) using peptide mass spectrometry approaches. Therefore, we used a series of IE62 deletion and peptide expression plasmids to map the ORF66-mediated phosphorylation of IE62. In previous studies, ORF66 induced the phosphorylation of a peptide of IE62 spanning residues 571 to 735, although much more efficient phosphorylation occurred with an IE62 peptide spanning residues 414 to 823 (30). The more efficient phosphorylation of the larger peptide was suspected to be a consequence of the presence of the predicted DNA binding and dimerization do-

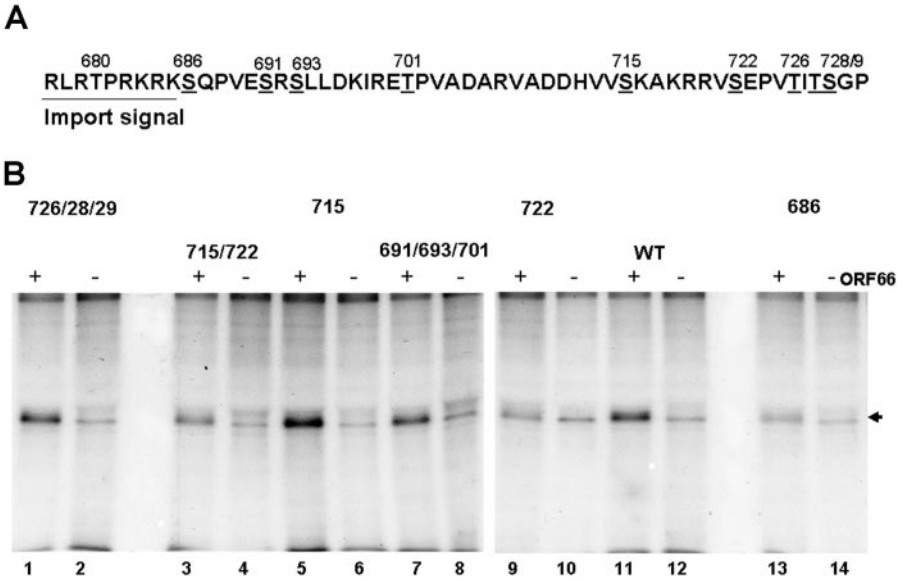

FIG. 4. Identification of ORF66-induced phosphorylation of IE62 peptides. (A) Representation of the region of IE62 containing ORF66-directed phosphorylation sites, with the amino acid sequence in single-letter code and the position of each serine or threonine residue indicated with the residue number above. (B) Radiograph showing SDS-PAGE-separated immunoprecipitates of ^{32}P-labeled IE62 peptides expressed in the absence (−) and presence (+) of a 1:1 ratio of functional ORF66 protein kinase. All peptides contain residues 414 to 735 of the IE62 peptide, but with specific serine/threonine transitions to alanine, as indicated above each pair of lanes. The arrowhead indicates the expected size of the phosphorylated IE62 peptides. Lane numbers are indicated at the bottom of the radiograph for reference in the text.

mains of IE62, which may act to stabilize the IE62 peptide in transfected cells. We therefore used a larger peptide, and deletions of it, as a basis for further mapping (Fig. 3A). Each HA-tagged IE62 peptide was coexpressed in transfected 293T cells with either functional untagged ORF66 protein kinase or an empty vector control, metabolically labeled with [^{32}P]orthophosphate, and immunoprecipitated with HA antibody. The immunoprecipitated IE62 peptide containing residues 414 to 735 expressed from plasmid pGK2-HA846 demonstrated strong phosphorylation in cells coexpressing the ORF66 protein kinase and little detectable phosphorylation in the absence of the kinase, confirming that this domain contained sites of ORF66-directed phosphorylation (Fig. 3B, lane 2). An IE62 peptide that contained an in-frame deletion of the residues between 571 and 656 (HA825) was also efficiently and preferentially phosphorylated in ORF66-coexpressing cells (Fig. 3B, lane 4). However, an IE62 peptide containing residues 414 to 571 fused to only the IE62 nuclear localization signal (HA819) did not show ^{32}P incorporation in ORF66-coexpressing or control cells (Fig. 3B, lane 6), and a peptide representing residues 414 to 687 (HA810) showed only minor labeling in both ORF66-expressing and control cells (lane 16). Notably, the HA810 peptide contains a predicted cdk2 consensus site at T680, and cdk2 regulates the nuclear import of SV40 T antigen (21). The implied phosphorylation of residues C terminal to the nuclear localization signal was strengthened by examining an IE62 peptide containing amino acids 414 to 571 fused to residues 673 to 735 (HA828), including T680, and a peptide containing residues 414 to 571 fused to residues 677 to 735 (HA811), which lacks the residues preceding T680 (Fig. 3B, lanes 14 and 12, respectively). Both of these peptides were efficiently phosphorylated, suggesting that ORF66-mediated phosphorylation events occur between residues 686 and 735, which are carboxyl to the IE62 NLS (Fig. 3A). In other studies, we noted that the HA810 peptide, terminating at residue 687, was not efficiently imported into the nucleus (data not shown). Since it was possible that the lack of phosphorylation of the peptide may have been a consequence of nuclear import, we examined two additional IE62 peptides in which the 414-571 peptide was fused to residues encoding the NLS from either ORF61 (HA821) or SV40 T antigen (HA823). These peptides were predominantly nuclear (data not shown), yet both were poor phosphorylation substrates (Fig. 3B, lanes 8 and 10). Thus, the differential phosphorylation events identified reflect the presence or absence of target motifs for phosphorylation rather than differences in cellular localization. Finally, it was possible that the observed phosphorylation differences could be due to unstable peptides, so we examined the expression of the peptides in transfected cells. All of the IE62 peptides used in this study were found to be efficiently expressed in transfected cell extracts, although we noticed a somewhat more efficient expression of most peptides in the presence of the kinase in some studies (Fig. 3C). However, the differences in expression do not account for the differences in phosphorylation seen in Fig. 3B, so we concluded that the different phosphorylation levels reflected the presence or absence of phosphorylation sites. We additionally noted that an ORF66-specific phosphorylated protein of approximately 17 kDa was found in many (Fig. 3B, lanes 2, 4, 6, 8, 10, and 16 [indicated by a hatched circle]), but not all (Fig. 3B, lanes 12 and 14), IE62 peptide immunoprecipitates from ORF66 kinase-positive cells. The identity of this protein has not yet been resolved.

To further delineate the ORF66-specific target residues within IE62, a site-specific mutagenesis approach was used, in

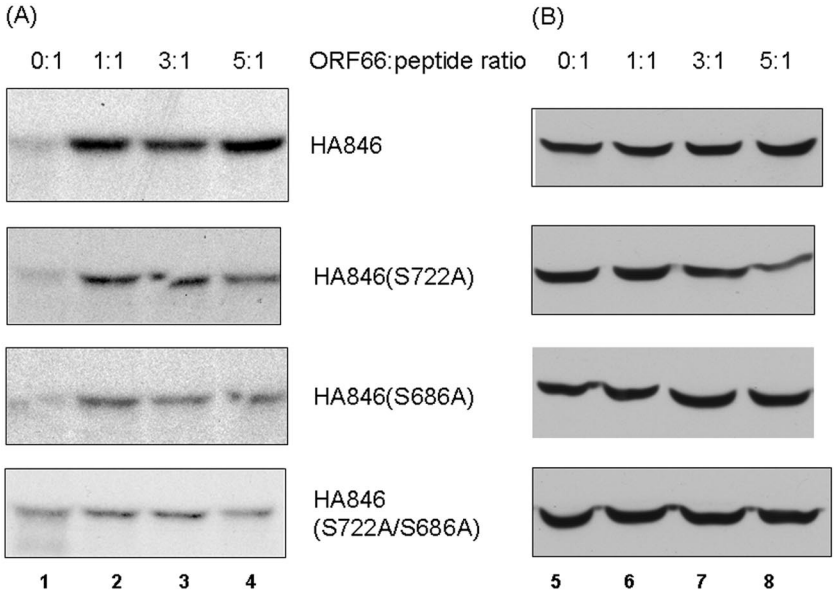

FIG. 5. Expression and [^{32}P]orthophosphate labeling of IE62 wild-type and serine mutant peptides expressed in the absence or presence of different levels of ORF66. (A) Autoradiograph showing SDS-PAGE-separated, [^{32}P]orthophosphate-labeled, immunoprecipitated peptides expressed from plasmid pGK2-HA846 (HA846) or similar plasmids with S686A, S722A, or S686A/S722A mutations. Immunoprecipitates were prepared from cells transfected with equal levels of plasmid expressing the IE62 peptide and with an empty vector or plasmid expressing ORF66, adjusted to give ORF66-to-IE62 peptide ratios of 0:1, 1:1, 3:1, and 5:1, as indicated at the top of the figure. The exposures of the autoradiographs were equivalent, except for that of the IE62 double mutant (S686A/S722A), which was overexposed approximately threefold compared to the others to show the minor level of phosphorylation by cellular kinases. (B) Immunoblots showing the expression of each HA-tagged IE62 peptide expressed in cells following similar transfections to those performed for panel A in order to show expression of the peptides at the different IE62 peptide-to-ORF66 ratios. The peptides were identified with HA-specific antibodies. Numbers at the bottom refer to lanes discussed in the text.

which single residues or clusters of the nine candidate threonine and serine residues between the IE62 NLS and amino acid 735 were mutated to alanine (Fig. 4A). Each point-mutated construct was generated in the background of the 414-735 peptide and then coexpressed and metabolically labeled in transfected 293T cells with either functional ORF66 protein kinase or a dead kinase expressed from the plasmid pCMV66-K122A (30). In this study, we detected a low level of IE62 peptide labeling in the absence of the functional ORF66 kinase, reflecting a weak activity of cellular protein kinases on the 414-735 peptide. This was also observed for the peptide expressed from construct 810 (Fig. 3B). In the presence of the ORF66 protein kinase, there was enhanced labeling of the wild-type peptide, as expected (Fig. 4B, lane 11). For peptides containing serine-to-alanine mutations of residues 691, 693, and 701 as a group and of residues 726, 728, and 729 as a group, there was ORF66-specific phosphorylation comparable to that of the wild-type peptide (Fig. 4B, lanes 1 and 7). However, for peptides that contained an S722A or S686A mutation, either alone or with other residues, there was a significant reduction in the level of phosphorylated peptides, although in no circumstance was all phosphorylation abrogated by a single point mutation. These results suggested that both S686 and S722 are target residues in IE62 for phosphorylation induced by the ORF66 protein kinase. Densitometric analysis of this experiment indicated that the S686A and S722A mutations abrogated 64% and 54% of IE62 peptide phosphorylation in the presence of the ORF66 kinase, respectively, compared to that of the unaltered peptide. Similar results were obtained with peptides expressed in transfected MeWo cells, although the level of basal phosphorylation of the peptides in the absence of the ORF66 kinase, presumably representing activities of cellular kinases, was found to be higher (data not shown).

To further evaluate the ORF66 protein kinase-induced phosphorylation at IE62 S686 and S722, we carried out in vivo labeling studies with peptides lacking one or both targets in the IE62 414-735 peptide background, using the wild-type peptide and S686A, S722A, and S686A/722A mutant peptides. MeWo cells were transfected at ORF66-to-IE62 plasmid ratios of 0:1, 1:1, 3:1, and 5:1 to determine if higher levels of phosphorylation could be achieved with more transfected kinase. The IE62 wild-type peptide exhibited an increase in phosphorylation of 3.7-fold at the 1:1 ratio over that of the peptide expressed under ORF66-negative conditions (0:1). At higher ratios of kinase to peptide, the level of phosphorylation did not increase significantly (Fig. 5A, peptide HA846). Peptides containing either the S722A or S686A single mutation exhibited an overall reduction in the level of phosphorylation when expressed with ORF66, although ORF66-induced phosphorylation was still apparent at all ratios of ORF66 to IE62 peptide compared to that with no kinase. In contrast, when both S686 and S722 were altered to alanine, IE62 peptide phosphorylation in the presence of ORF66 was reduced to the background phosphorylation levels seen in the absence of transfected ORF66. Densitometric analysis of the level of phosphorylation of the double mutant IE62 peptide indicated only a 1.3-fold increase in phosphorylation at the 1:1 and 3:1 ratios and no relative phosphorylation increase at the 5:1 ratio compared to that of the peptide expressed in the absence of ORF66 (0:1). Immunoblot ana-

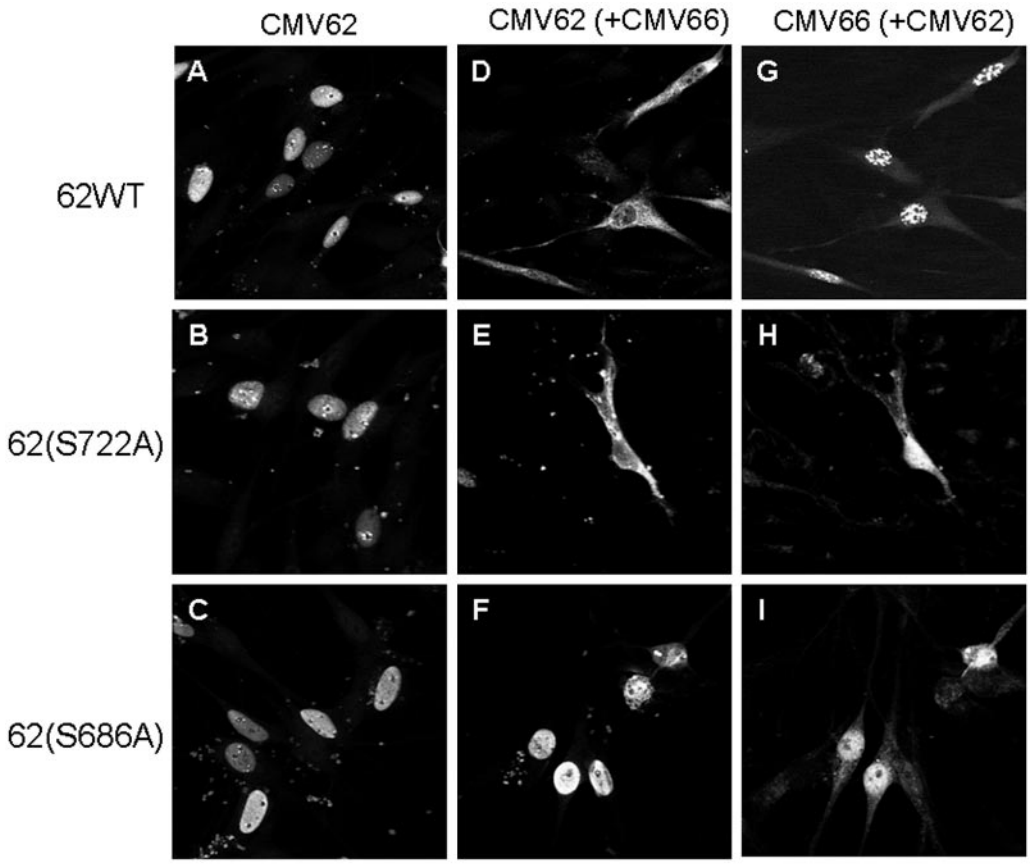

FIG. 6. IE62 protein containing S686A, but not S722A, mutation is resistant to ORF66-mediated nuclear exclusion. IE62 proteins carrying either the wild-type residues or an S686A or S722A mutation were expressed in the presence or absence of functional HA-tagged ORF66 in VZV-permissive MeWo cells, and their cellular distributions were determined using indirect immunofluorescence at 24 h, as described in Materials and Methods. IE62 was detected using rabbit anti-IE62 with secondary Alexa fluor 488-conjugated antibodies, and ORF66 was detected using mouse anti-HA with secondary Alexa fluor 546-conjugated antibodies. The left panels exhibit full-length IE62 proteins transfected in the absence of ORF66 (A to C), the middle panels display IE62 protein staining in cells coexpressing the live HA-tagged ORF66 kinase (D to F), and the right panels (G to I) show the expression of HA-tagged ORF66 in the same cells as those shown in the middle panels.

lyses of the IE62 peptides expressed in transfected cells with different levels of the protein kinase indicated that they were efficiently expressed (Fig. 5B). Overall, the differences shown in Fig. 5A were concluded to reflect ^{32}P incorporation levels and not peptide expression levels. These data support the conclusion that ORF66-mediated phosphorylation of the IE62 peptide is largely restricted to two sites carboxyl to the IE62 NLS, namely, residues S686 and S722.

Identification of ORF66-induced phosphorylation events affecting nuclear import of IE62. Both IE62 residues S686 and S722 are carboxyl to the mapped NLS of IE62 (30, 33) and have similarities in contextual sequence (Fig. 4A). Both are preceded by three basic amino acids, at the −4, −3, and −2 positions, and are followed by a proline at the +2 position and a valine at the +3 position. Interestingly, only the arginine/lysine-rich region preceding S686 acts as an NLS in MeWo cells (33). If phosphorylation of IE62 at S686 (immediately adjacent to the NLS) or S722 (37 residues downstream of the NLS) affects IE62 nuclear import, then alteration of the key target serine should result in the generation of a nuclear IE62 protein in the presence of the ORF66 kinase. To this end, the cellular distributions of wild-type and mutant full-length IE62 proteins containing serine-to-alanine mutations were analyzed (Fig. 6). In these studies, functional, HA-tagged ORF66 kinase was used to facilitate the identification and cellular localization of the protein kinase in transfected cells by immunofluorescence. All cotransfections were performed at a 1:1 ratio of ORF66 to IE62. Two hundred IE62-positive cells were scored for the cellular distribution of IE62 under each condition.

Full-length, wild-type IE62 expressed in the absence of ORF66 showed typical nuclear localization in >94% of IE62-positive cells, with diffuse nuclear staining, negative nucleolar staining, and subnuclear concentrations in distinct dots adjacent to the nucleolus (Fig. 6A). Rare cells (<5% of the total positive cells) showed some cytoplasmic distribution of IE62, and these were suspected to represent cells with poorly defined nuclear membranes that may have recently undergone cell division. Only 1 cell of 200 counted showed an exclusively cytoplasmic form of IE62. Virtually identical nuclear distribution patterns were found for IE62 S686A (Fig. 6B) and IE62 S722A (Fig. 6C) mutant proteins in the absence of ORF66 kinase expression. In the presence of the ORF66 kinase, approximately 70% of the wild-type IE62-positive cells demonstrated predominantly cytoplasmic staining of the IE62 pro-

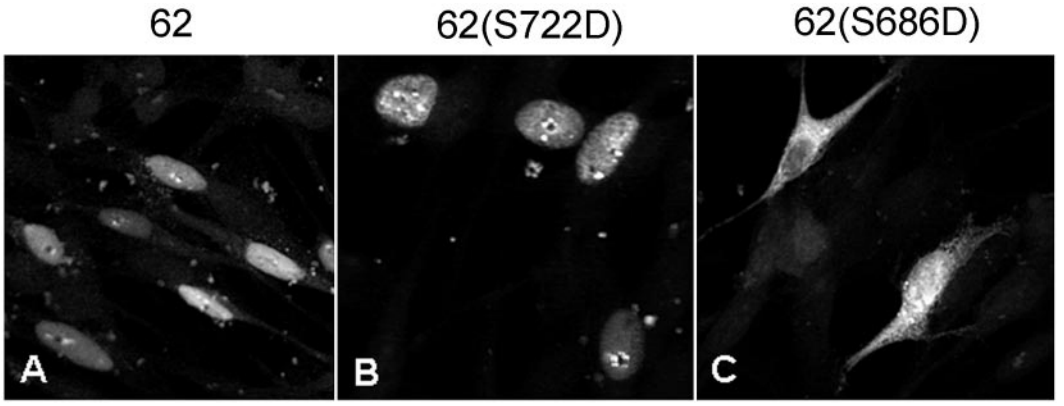

FIG. 7. Mimicking phosphorylation through aspartic acid replacement of S686, but not S722, results in partial inhibition of nuclear import. Full-length IE62 proteins with the wild-type sequence or with an S686D or S722D mutation were individually transfected into MeWo cells, and cells were fixed and stained for IE62 expression using anti-IE62 and Alexa fluor 488-conjugated secondary antibodies as described in Materials and Methods. Representative cells are shown. The specific S→D mutation is indicated above each panel.

tein, with the remaining cells demonstrating both nuclear and cytoplasmic forms of IE62 (Fig. 6D). No cells expressing both wild-type IE62 and ORF66 demonstrated a predominantly nuclear phenotype for the IE62 protein, and nuclear IE62 was only detected in those few transfected cells which failed to coexpress ORF66. The ORF66 protein demonstrated a predominantly nuclear speckled localization in many cells in the presence of wild-type IE62, with some cytoplasmic distribution, similar to that observed in previous studies (30). Like wild-type IE62, IE62 containing the S722A mutation coexpressed with the ORF66 protein kinase resulted in predominantly cytoplasmic localization of the IE62 protein in all ORF66-coexpressing cells (Fig. 6E). In contrast, IE62 carrying the S686A mutation demonstrated predominantly nuclear localization in both the presence and the absence of the ORF66 protein kinase in nearly all cells, similar to wild-type IE62 expressed alone (Fig. 6C and F). The ORF66 kinase showed a mostly nuclear distribution but nucleolar exclusion, and confocal analyses indicated a predominant overlap of the signals of the two proteins. The IE62 S686A mutant protein remained nuclear even in the presence of high ratios of ORF66 to IE62, suggesting that the kinase insensitivity of nuclear localization could not be overcome by expressing higher levels of protein kinase (data not shown). These results strongly suggest that ORF66-mediated phosphorylation of S686 is the event that causes the cytoplasmic accumulation of IE62.

To further support this interpretation, we derived and expressed IE62 proteins that contained the S686D or S722D mutation, designed to place a permanent, primary structure-based negative charge at S686 or S722, to mimic the negative charges exerted by phosphorylation. In transfected MeWo cells, the IE62 S722D protein showed a nuclear distribution similar to that of the wild-type protein, including subnuclear concentrations adjacent to nucleoli (Fig. 7B). In contrast, the IE62 S686D protein demonstrated inefficient nuclear import, with most cells displaying at least some cytoplasmic accumulation. Some cells expressing the IE62 S686D protein had little nuclear distribution (Fig. 7C, upper left), but many demonstrated some nuclear accumulation with obvious cytoplasmic accumulation (Fig. 7C, lower right). Confocal sectioning indicated that there was nuclear import of the IE62 S686D protein in these cells. These results are consistent with the ORF66-mediated phosphorylation and addition of a negative charge at IE62 residue S686, which negatively regulates the activity of the immediately adjacent NLS. The partially inhibited nuclear import phenotype likely resulted from the inability of the aspartate residue to fully mimic the negative charge exerted by phosphorylation.

Baculovirus-mediated expression and in vitro autophosphorylation of ORF66 kinase. The observed phosphorylation of IE62 in ORF66-expressing cells could be either a consequence of direct phosphorylation by the ORF66 kinase or the result of an indirect mechanism, such as ORF66 activation of a cellular kinase or pathway that leads to IE62 phosphorylation. We therefore considered it necessary to determine if the ORF66 kinase could directly phosphorylate IE62. Extensive attempts to develop an in vitro kinase assay with ORF66 obtained from VZV-infected cells were not successful, because the ORF66 protein kinase has proven to be highly insoluble in buffers designed to solubilize the kinase and retain its kinase activity. Therefore, we expressed the HA-tagged ORF66 protein kinase in SF9 cells by using a recombinant baculovirus (Bac-HA66). Following a high-multiplicity infection and 48 h of expression, approximately 5% of the total HA-ORF66 protein was soluble after cell lysis in a mild RIPA buffer. Immunoblotting of HA-ORF66 with HA-specific antibodies resulted in the identification of two closely migrating but distinct forms on SDS-PAGE gels, as seen for transfected cells (30; data not shown).

We first examined autophosphorylation of the SF9-expressed protein kinase. ORF66 autophosphorylation was implied from the observation that point-inactivated ORF66 kinases do not exhibit the slower migrating form on SDS-PAGE gels (30). Extracts of SF9 cells expressing either the HA-ORF66 kinase or the GST control were immunoprecipitated with HA-specific or nonspecific antibodies in either the presence or absence of a blocking HA peptide or an unrelated peptide. The washed immunoprecipitates were incubated with a standard kinase buffer containing 10 mM $MgCl_2$, [γ-^{32}P]ATP, and 10 μg/ml heparin (to block casein kinase II activity) (45).

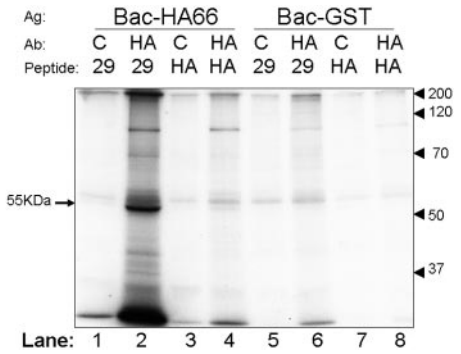

FIG. 8. Development of immunocomplexed ORF66 in vitro kinase assay. Protein antigens (Ag) from SF9 insect cells infected with Bac-HA66 or control Bac-GST were solubilized in a modified RIPA buffer and immunoprecipitated with either anti-HA (HA) or a nonspecific (C) antibody in the presence of either 0.2 mg/ml specific (HA) or nonspecific (29) competitor peptide. Washed immunoprecipitates were then incubated with [γ-^{32}P]ATP in kinase buffer as described in Materials and Methods. Proteins were resolved by SDS-PAGE and detected by autoradiography. SDS-PAGE standards are marked at the right, and lanes are marked at the bottom of each panel for reference in the text. The 55-kDa HA-ORF66 autophosphorylated protein band is indicated by an arrow to the left of the autoradiograph.

This buffer was found through preliminary studies not to affect ORF66 kinase activity. SDS-PAGE and autoradiography revealed a heavily phosphorylated band of 55 kDa, consistent with the size of HA-tagged ORF66, only in immunoprecipitates from SF9 cells infected with Bac-HA66 (Fig. 8, lane 2). This band was efficiently detected when a nonspecific peptide was used with the antibody-antigen mix, and its immunoprecipitation was inhibited by the addition of HA peptide (Fig. 8, lane 4). There was no equivalent 55-kDa phosphorylated band in extracts immunoprecipitated from Bac-GST-infected cells under any conditions (Fig. 8, lanes 5 to 8). These data show that the HA-ORF66 kinase is specifically precipitated from Bac-HA66-infected cell extracts and can autophosphorylate.

The optimal conditions for ORF66 in vitro kinase activity were determined by evaluating cation choice (Mn^{2+} or Mg^{2+}) and concentrations (2 to 100 mM), different pHs (pH 6.0 to 9.0), and various salt concentrations (0 to 1 M KCl). These were examined for autophosphorylation activities, but the optimal conditions were found to be suitable for transphosphorylation of a highly purified IE62-MBP 571-735 peptide. Kinase activity was found to be optimal with 50 mM Mn^{2+}, physiological pH (7.5), and 50 mM KCl and was not inhibited by 10 μg/ml heparin. As such, the optimized buffer was used for all remaining kinase assays. We note that the preference for Mn^{2+} ions was also found for the phosphorylation activity of the VZV ORF47 kinase (45). While sites for autophosphorylation of ORF66 have not yet been determined, two ORF66 candidate sequences (KRS_{331}SRKPGSR and RHRPS_{368}) have serines proximal to multiple basic residues, as found for the target residues for ORF66-directed phosphorylation in IE62.

ORF66 phosphorylates IE62 peptides in vitro with the same specificity as in vivo. To determine if ORF66 could directly phosphorylate IE62, immunoconjugated HA-ORF66 was incubated with purified MBP-IE62 peptide fusion substrates under optimal kinase conditions (Fig. 9). Four purified MBP fusion proteins containing IE62 amino acids 571 to 735 fused to MBP were analyzed, with or without changes at the specific serine residues identified in the in vivo phospholabeling studies (wild type, S686A, S722A, and S686A/S722A; Fig. 9A). Equal amounts of these fusion proteins (Fig. 9B, lanes 11 to 14) were incubated with HA immunoprecipitates from Bac-HA66 (Fig. 9B, lanes 1 to 5)- or Bac-GST-infected cell lysates (Fig. 9B, lanes 6 to 10) and analyzed by SDS-PAGE. In the Bac-GST control immunoprecipitates, virtually no phosphate labeling was detected for any of the IE62 peptides (Fig. 9B, lanes 6 to 10; the first and second panels represent equally exposed autoradiographs). However, incubation of MBP-IE62 fusion proteins with Bac-HA66 immunoprecipitates resulted in strong phosphorylation of the wild-type MBP-IE62 fusion (Fig. 9B, lane 1). Importantly, the MBP-IE62 fusion with point mutations at both S686 and S722 was a much poorer substrate for the HA-ORF66 kinase, despite loading of equivalent levels of each MBP-IE62 peptide. Furthermore, individual mutations of one serine to an alanine resulted in reduced phosphorylation of the peptides, but not to the extent of wild-type IE62-MBP fusions (Fig. 9B, lanes 3 and 4). The phosphorylated protein of 55 kDa was the autophosphorylated protein kinase, as it was present in the immunoprecipitates lacking any MBP fusions and was not present in Bac-GST control immunoprecipitates. Similar results were obtained for two replicate experiments.

Phosphorimaging analysis of phosphorylated MBP-IE62 peptides was performed for three replicate experiments, and the average percent optical density (compared to that of the wild type) of each phosphorylated band is plotted in Fig. 9C. A marked (~75%) decrease in signal was observed with the double mutant peptide, and a reduced signal was seen with a single mutation of either S686 or S722 individually. We concluded that IE62 is a direct substrate for the ORF66 protein kinase and that the activity observed in our in vitro reactions reflects a direct ORF66-mediated IE62 phosphorylation event. Thus, IE62 represents a new target for the US3 group of kinases.

DISCUSSION

Taken together with previous results (29, 30, 33), our results have now shown that VZV IE62, the principal transcriptional transactivator and a major component of the VZV virion tegument, is a direct target for phosphorylation by the VZV ORF66 protein kinase. Phosphorylation occurs at two residues, but the targeting of residue S686 is sufficient to induce IE62 to become cytoplasmic. These observations are consistent with a model in which one role of the ORF66 protein kinase is to directly phosphorylate IE62, negating its nuclear import to possibly negatively regulate IE62-mediated transcriptional activation of viral gene expression and/or to potentially enable virion inclusion of a preformed transactivator in the VZV virion tegument. Since ORF66-negative viruses are impaired for growth in T lymphocytes and in the SCID-hu thy/liv model of VZV infection (40, 55, 57), the interaction of ORF66 with IE62 may be important for efficient viral pathogenesis.

Several lines of evidence were presented to support the conclusion that the ORF66 protein kinase phosphorylates IE62. Previously, nuclear exclusion of the IE62 protein by the ORF66 protein was shown to occur only if the protein kinase

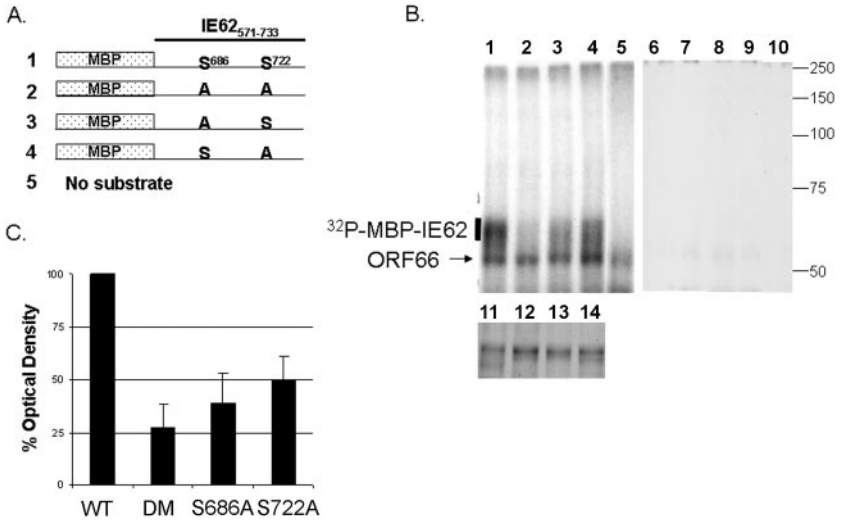

FIG. 9. Immunopurified ORF66 specifically phosphorylates MBP-IE62 peptides at S686 and S722 in vitro. (A) Representation of MBP-IE62 fusion proteins that were constructed and purified for the in vitro kinase assay. The residues at positions 686 and 722 are shown in single-letter code for the IE62 portion of the fusion peptide. (B) Autoradiographs of in vitro kinase assays using equivalent amounts of each purified MBP-IE62 substrate protein shown in panel A. The purified proteins were incubated in optimal kinase buffer with immunocomplexed HA-ORF66 (lanes 1 to 5) or with similar HA-tagged immunoprecipitates obtained from Bac-GST-infected cell lysates (lanes 6 to 10). Lanes 1 and 6 contain the wild-type IE62 peptide, lanes 2 and 7 contain the double mutant peptide, lanes 3 and 8 contain the S686A mutant peptide, lanes 4 and 9 contain the S722A mutant peptide, and lanes 5 and 10 contain the respective baculovirus immunoprecipitates with no added maltose binding protein fusions. Both autoradiographs were exposed equally. The lower panel (lanes 11 to 14) shows SDS-PAGE-separated input MBP-IE62 substrate proteins used for lanes 1 to 4 and 6 to 10 following staining with Coomassie brilliant blue to show the purified proteins. To the right of the radiographs are shown the approximate positions of molecular mass markers, in kDa. (C) Average values from densitometric quantification of autoradiographs of three replicate experiments, including that shown in panel B. Densitometric values of phosphorylated MBP-IE62 fusion proteins were normalized to the wild-type MBP-IE62 peptide densitometry value (set to 100%) after subtracting the background signal for each lane. Error bars represent standard deviations from the means. Only the region of the gel indicated by a bar to the left of the autoradiograph in panel B was evaluated. DM, double mutant.

activity of ORF66 was intact, and this correlated with enhanced phosphorylation of IE62 peptides by the ORF66 kinase in the context of both transfection and VZV infection (30). In a second study, IE62 demonstrated slightly different mobilities in SDS-PAGE gels if the ORF66 kinase was not expressed (29). Here we used tryptic phosphopeptide mapping studies to further establish that ORF66 directs new phosphorylation events in full-length IE62, in both cotransfections and VZV infections. Two novel IE62 phosphopeptides were observed when IE62 was coexpressed with ORF66 transiently, and one IE62 phosphopeptide spot that was abundant in both ROka and ROka47S IE62 peptide maps was considerably reduced for IE62 from ROka66S. These differential levels of phosphopeptide spots do not discriminate between direct phosphorylation and ORF66-induced cellular kinase activity. We also noted an overall reduction in many other IE62 phosphopeptides found in the presence of ORF66, although they migrated to the same relative positions. One possible reason for the reduction is that IE62 is phosphorylated by compartmentalized cellular kinases, which act differentially on IE62 as a result of the ORF66-induced cellular relocalization of IE62. Another possibility is that ORF66 activates host cell signaling cascades and the activities of cellular kinases that subsequently lead to an increased level of IE62 phosphorylation. Other alphaherpesvirus US3 kinases have been implicated in affecting host signaling cascades because they have multiple effects on host cell function, such as multiple cytoskeletal reorganization effects (14, 56, 61). Studies are currently under way to determine the general phosphoprotein state of cells expressing the ORF66 kinase.

IE62 peptides demonstrated the same phosphorylation specificities in both in vivo phospho-labeling studies in the presence of ORF66 and in vitro ORF66 kinase assays, strongly suggesting that IE62 is a direct target. Individually mutated IE62 peptides with the S686A or S722A mutation showed reduced phosphorylation, and mutation of both residues resulted in peptides that were much less sensitive to ORF66 phosphorylation. For an intermediate cellular kinase to act as the go-between for ORF66-mediated phosphorylation of IE62, it would have to efficiently copurify with the baculovirus-expressed immunopurified ORF66 and have activity in the same buffer used for the kinase assays. The use of the divalent cation Mn^{2+} and heparin excludes the activity of contaminating cellular casein kinase II, and we believe that other cellular kinase contamination is highly unlikely. Further proof will require high-level purification of the ORF66 protein kinase and a demonstration of its affinity for its substrates. A suitable approach for this was recently elegantly demonstrated with the HSV-1 US3 kinase, in which an active purified GST-US3 protein specifically phosphorylated several viral and cellular target-MBP protein fusion substrates (24). For ORF66, this has proven to be quite difficult because the protein kinase from VZV-infected cells is very insoluble, and we have found that a GST addition to the N terminus of ORF66 appears to inactivate or interfere with the kinase activity of ORF66 (A. Erazo,

K. Fite, and P. R. Kinchington, unpublished data). Nevertheless, strategies to purify ORF66 may enable a more rigorous in vitro phosphorylation assay to be developed.

Of the two IE62 residues phosphorylated by ORF66, only S686 was shown to be involved in the nuclear exclusion of IE62. In conventional nuclear import, a basic arginine/lysine-rich NLS is recognized by one or more of the six importin α proteins, which in turn complex with importin β and are translocated through the nuclear pore via the GTP-binding protein Ran (reviewed in references 23 and 43). IE62 S686 is immediately adjacent to the IE62 NLS (amino acids 677 to 685) (33), and the close proximity strongly suggests an underlying mechanism in which phosphorylation inhibits nuclear import. The nuclear import of many proteins is highly regulated by phosphorylation close to their NLSs (reviewed in references 16 and 22). Recent studies have shown that either direct phosphorylation or mutations mimicking phosphorylation through acidic residue replacement of the target residue at a site immediately N-terminal to an NLS result in a decreased affinity of the NLS for importin α (16). N-terminal phosphorylation events that impair the nuclear import of proteins are common and occur in proteins such as SV40 T antigen, parathyroid hormone-related protein, and v-Jun (21, 37, 53, 60). As far as we know, IE62 is one of a much rarer group of proteins that are nuclear import regulated by phosphorylation at a residue carboxyl to the NLS. One other such protein is the adenomatous polyposis coli protein (65). Mechanistically, the simplest explanation is that the strong negative charge exerted by phosphorylation at a site proximal to the NLS reduces the importin binding affinity. However, there are some suggestions that more complex issues affect the nuclear distribution of IE62. In transfected cells, the majority of ORF66 protein localizes to the nucleus, with only a fraction remaining cytoplasmic. With the simple model, phosphorylation of newly translated IE62 at S686 would be mediated by the small fraction of cytoplasmic ORF66. In an alternative explanation, the phosphorylation of IE62 by ORF66 would occur in the nucleus, and coupled with a possible nuclear export mechanism of phosphorylated IE62, IE62 would exit and be unable to reenter the nucleus. In a VZV infection, the latter scenario would enable nuclei to become empty of IE62 at late stages of VZV infection, and we and others have observed that many late-stage nuclei in wild-type VZV plaques appear devoid of IE62 (unpublished data; also see the figures in reference 4). The possible nucleocytoplasmic shuttling capability of IE62 in VZV infection is currently under investigation.

The functional significance of phosphorylation at residue S722 is not yet clear. While residues immediately amino terminal to S722 have similarity to canonical NLSs (Fig. 4A), the sequence cannot act as an NLS in the absence of the 677-685 NLS sequence in MeWo cells (33). Furthermore, phosphorylation of S722 (in S686A mutants of IE62) did not inhibit IE62 nuclear import in the multiple cell types tested. However, we postulate that the IE62 716-720 basic-residue region may function as an NLS in a specific cell type(s) that has not yet been identified. The six known importin α proteins each demonstrate variable binding specificities for cargoes and also show cell-type-dependent regulation of expression (43, 51). VZV infects multiple cell types during the natural course of infection, including epithelial cells, T lymphocytes, dendritic cells (42), skin cells, and sensory neurons (35, 36), and it is possible that the IE62 716-720 region may be a functional or preferred NLS in one of these cell types. Therefore, we suggest that the phosphorylation of both S686 and S722 is maintained to abrogate IE62 nuclear import at later stages of VZV infection in multiple host cell types with different importin α expression characteristics.

IE62 is the first viral target reported for the VZV ORF66 kinase, and the corresponding interaction demonstrated in this work has not been reported for other alphaherpesviruses. We previously postulated that IE62's role as a tegument protein may be partly to supplement transactivation of IE viral gene expression (31), as a VZV that does not express ORF10, the HSV-1 VP16 homolog, can still grow well in culture (8). Several viral targets of the orthologous US3 kinase have been identified, but it is not yet clear whether these are conserved in VZV. While ORF66 is not "essential" for tissue culture growth, disruption of ORF66 expression results in low virus production and poor capsid assembly (55). Recent data suggest that ORF66 may affect additional functions in the host cell in addition to those of IE62. ORF66 induces the downregulation of major histocompatibility complex class I surface expression (1; A. J. Eisfeld and P. R. Kinchington, unpublished data). In addition, a comparison of ORF66-expressing and non-ORF66-expressing viruses in T cells has suggested that ORF66 may have roles in resistance to interferon as well as the inhibition of virally induced apoptosis (55). Both of these activities have been attributed to US3 protein kinases (44, 46, 50). It thus seems that US3 kinases may share some common host cell targets but that viral targets have differentiated as VZV and other alphaherpesviruses have evolved and separated from a presumed common ancestor. The effects of ORF66 on the host cell are now under investigation.

ACKNOWLEDGMENTS

This work was supported by Public Health Service grant EY09397, a CORE grant for Vision Research (EY08098), funds from the Eye & Ear Foundation and from Research to Prevent Blindness, Inc., and a Lew Wasserman award to P.R.K. A.J.E. was supported by predoctoral T32 training grant AI49820.

We thank Thomas Smithgall of the University of Pittsburgh for the use of a two-dimensional electrophoresis system.

REFERENCES

1. **Abendroth, A., I. Lin, B. Slobedman, H. Ploegh, and A. M. Arvin.** 2001. Varicella-zoster virus retains major histocompatibility complex class I proteins in the Golgi compartment of infected cells. J. Virol. **75:**4878–4888.
2. **Baudoux, L., P. Defechereux, S. Schoonbroodt, M. P. Merville, B. Rentier, and J. Piette.** 1995. Mutational analysis of varicella-zoster virus major immediate-early protein IE62. Nucleic Acids Res. **23:**1341–1349.
3. **Besser, J., M. Ikoma, K. Fabel, M. H. Sommer, L. Zerboni, C. Grose, and A. M. Arvin.** 2004. Differential requirement for cell fusion and virion formation in the pathogenesis of varicella-zoster virus infection in skin and T cells. J. Virol. **78:**13293–13305.
4. **Besser, J., M. H. Sommer, L. Zerboni, C. P. Bagowski, H. Ito, J. Moffat, C. C. Ku, and A. M. Arvin.** 2003. Differentiation of varicella-zoster virus ORF47 protein kinase and IE62 protein binding domains and their contributions to replication in human skin xenografts in the SCID-hu mouse. J. Virol. **77:** 5964–5974.
5. **Boyle, W. J., P. Van de Geer, and T. Hunter.** 1991. Phosphopeptide mapping and phosphoamino acid analysis by two-dimensional separation on thin-layer cellulose plates. Methods Enzymol. **201:**110–149.
6. **Carrozza, M. J., and N. A. DeLuca.** 1996. Interaction of the viral activator protein ICP4 with TFIID through TAF250. Mol. Cell. Biol. **16:**3085–3093.
7. **Cohen, J. I., D. Heffel, and K. Seidel.** 1993. The transcriptional activation domain of varicella-zoster virus open reading frame 62 protein is not conserved with its herpes simplex virus homolog. J. Virol. **67:**4246–4251.

8. **Cohen, J. I., and K. Seidel.** 1994. Varicella-zoster virus (VZV) open reading frame 10 protein, the homolog of the essential herpes simplex virus protein VP16, is dispensable for VZV replication in vitro. J. Virol. **68:**7850–7858.
9. **Cohrs, R. J., D. H. Gilden, P. R. Kinchington, E. Grinfeld, and P. G. E. Kennedy.** 2003. Varicella-zoster virus gene 66 transcription and translation in latently infected human ganglia. J. Virol. **77:**6660–6665.
10. **Disney, G. H., and R. D. Everett.** 1990. A herpes simplex virus type 1 recombinant with both copies of the Vmw175 coding sequences replaced by the homologous varicella-zoster virus open reading frame. J. Gen. Virol. **71:**2681–2689.
11. **Disney, G. H., T. A. McKee, C. M. Preston, and R. D. Everett.** 1990. The product of varicella-zoster virus gene 62 autoregulates its own promoter. J. Gen. Virol. **71:**2999–3003.
12. **Felser, J. M., P. R. Kinchington, G. Inchauspe, S. E. Straus, and J. M. Ostrove.** 1988. Cell lines containing varicella-zoster virus open reading frame 62 and expressing the "IE" 175 protein complement ICP4 mutants of herpes simplex virus type 1. J. Virol. **62:**2076–2082.
13. **Forghani, B., R. Mahalingam, A. Vafai, J. W. Hurst, and K. W. Dupuis.** 1990. Monoclonal antibody to immediate early protein encoded by varicella-zoster virus gene 62. Virus Res. **16:**195–210.
14. **Geenen, K., H. W. Favoreel, L. A. Olsen, L. W. Enquist, and H. J. Nauwynck.** 2005. The pseudorabies virus US3 protein kinase possesses anti-apoptotic activity that protects cells from apoptosis during infection and after treatment with sorbitol or staurosporine. Virology **331:**144–150.
15. **Grinfeld, E., and P. G. E. Kennedy.** 2004. Translation of varicella-zoster virus genes during human ganglionic latency. Virus Genes **29:**317–319.
16. **Harreman, M. T., T. M. Kline, H. G. Milford, M. B. Harben, A. E. Hodel, and A. H. Corbett.** 2004. Regulation of nuclear import by phosphorylation adjacent to nuclear localization signals. J. Biol. Chem. **279:**20613–20621.
17. **Heineman, T. C., and J. I. Cohen.** 1995. The varicella-zoster virus (VZV) open reading frame 47 (ORF47) protein kinase is dispensable for viral replication and is not required for phosphorylation of ORF63 protein, the VZV homolog of herpes simplex virus ICP22. J. Virol. **69:**7367–7370.
18. **Heineman, T. C., K. Seidel, and J. I. Cohen.** 1996. The varicella-zoster virus ORF66 protein induces kinase activity and is dispensable for viral replication. J. Virol. **70:**7312–7317.
19. **Honess, R. W., and B. Roizman.** 1974. Regulation of herpesvirus macromolecular synthesis. I. Cascade regulation of the synthesis of three groups of viral proteins. J. Virol. **14:**8–19.
20. **Honess, R. W., and B. Roizman.** 1975. Regulation of herpesvirus macromolecular synthesis: sequential transition of polypeptide synthesis requires functional viral polypeptides. Proc. Natl. Acad. Sci. USA **72:**1276–1280.
21. **Jans, D. A., M. J. Ackermann, J. R. Bischoff, D. H. Beach, and R. Peters.** 1991. p34cdc2-mediated phosphorylation at T124 inhibits nuclear import of SV-40 T antigen proteins. J. Cell Biol. **115:**1203–1212.
22. **Jans, D. A., and S. Hubner.** 1996. Regulation of protein transport to the nucleus: central role of phosphorylation. Physiol. Rev. **76:**651–685.
23. **Jans, D. A., C. Y. Xiao, and M. H. Lam.** 2000. Nuclear targeting signal recognition: a key control point in nuclear transport? Bioessays **22:**532–544.
24. **Kato, A., M. Yamamoto, T. Ohno, H. Kodira, Y. Nishiyama, and Y. Kawaguchi.** 2005. Identification of proteins phosphorylated directly by the US3 protein kinase encoded by herpes simplex virus type 1. J. Virol. **79:**9325–9331.
25. **Kennedy, P. G. E.** 2002. Key issues in varicella-zoster virus latency. J. Neurovirol. **8:**80–84.
26. **Kenyon, T. K., J. Lynch, J. Hay, W. Ruyechan, and C. Grose.** 2001. Varicella-zoster virus ORF47 protein serine kinase: characterization of a cloned, biologically active phosphotransferase and two viral substrates, ORF62 and ORF63. J. Virol. **75:**8854–8858.
27. **Kinchington, P. R., D. Bookey, and S. E. Turse.** 1995. The transcriptional regulatory proteins encoded by varicella-zoster virus open reading frames (ORFs) 4 and 63, but not ORF 61, are associated with purified virus particles. J. Virol. **69:**4274–4282.
28. **Kinchington, P. R., and J. I. Cohen.** 2000. Varicella zoster virus proteins, p. 74–104. *In* A. M. Arvin and A. A. Gershon (ed.), Varicella zoster virus: virology and clinical management. Oxford Press, Oxford, United Kingdom.
29. **Kinchington, P. R., K. Fite, A. Seman, and S. E. Turse.** 2001. Virion association of IE62, the varicella-zoster virus (VZV) major transcriptional regulatory protein, requires expression of the VZV open reading frame 66 protein kinase. J. Virol. **75:**9106–9113.
30. **Kinchington, P. R., K. Fite, and S. E. Turse.** 2000. Nuclear accumulation of IE62, the varicella-zoster virus (VZV) major transcriptional regulatory protein, is inhibited by phosphorylation mediated by the VZV open reading frame 66 protein kinase. J. Virol. **74:**2265–2277.
31. **Kinchington, P. R., J. K. Hougland, A. M. Arvin, W. T. Ruyechan, and J. Hay.** 1992. The varicella-zoster virus immediate-early protein IE62 is a major component of virus particles. J. Virol. **66:**359–366.
32. **Kinchington, P. R., G. Inchauspe, J. H. Subak-Sharpe, F. Robey, J. Hay, and W. T. Ruyechan.** 1988. Identification and characterization of a varicella-zoster virus DNA-binding protein by using antisera directed against a predicted synthetic oligopeptide. J. Virol. **62:**802–809.
33. **Kinchington, P. R., and S. E. Turse.** 1998. Regulated nuclear localization of the varicella zoster virus major regulatory protein IE62. J. Infect. Dis. **178:** S16–S21.
34. **Ku, C. C., J. Besser, A. Abendroth, C. Grose, and A. M. Arvin.** 2005. Varicella-zoster virus pathogenesis and immunobiology: new concepts emerging from investigations with the SCIDhu mouse model. J. Virol. **79:** 2651–2658.
35. **Ku, C. C., L. Zerboni, H. Ito, and A. Arvin.** 2003. Varicella-zoster virus pathogenesis: viral transfer to skin in CD4+ T lymphocytes and evasion of IFN-alpha. FASEB J. **17:**C154.
36. **Ku, C. C., L. Zerboni, H. Ito, B. S. Graham, M. Wallace, and A. M. Arvin.** 2004. Varicella-zoster virus transfer to skin by T cells and modulation of viral replication by epidermal cell interferon-alpha. J. Exp. Med. **200:**917–925.
37. **Lam, M. H., L. J. Briggs, W. Hu, T. J. Martin, M. T. Gillespie, and D. A. Jans.** 1999. Importin beta recognizes parathyroid hormone-related protein with high affinity and mediates its nuclear import in the absence of importin alpha. J. Biol. Chem. **274:**7391–7398.
38. **Lungu, O., C. A. Panagiotidis, P. W. Annunziato, A. A. Gershon, and S. J. Silverstein.** 1998. Aberrant intracellular localization of varicella-zoster virus regulatory proteins during latency. Proc. Natl. Acad. Sci. USA **95:**7080–7085.
39. **Lynch, J. M., T. K. Kenyon, C. Grose, J. Hay, and W. T. Ruyechan.** 2002. Physical and functional interaction between the varicella zoster virus IE63 and IE62 proteins. Virology **302:**71–82.
40. **Moffat, J. F., L. Zerboni, M. H. Sommer, T. C. Heineman, J. I. Cohen, H. Kaneshima, and A. M. Arvin.** 1998. The ORF47 and ORF66 putative protein kinases of varicella-zoster virus determine tropism for human T cells and skin in the SCID-hu mouse. Proc. Natl. Acad. Sci. USA **95:**11969–11974.
41. **Moriuchi, M., H. Moriuchi, S. E. Straus, and J. I. Cohen.** 1994. Varicella-zoster virus (VZV) virion-associated transactivator open reading frame 62 protein enhances the infectivity of VZV DNA. Virology **200:**297–300.
42. **Morrow, G., B. Slobedman, A. L. Cunningham, and A. Abendroth.** 2003. Varicella-zoster virus productively infects mature dendritic cells and alters their immune function. J. Virol. **77:**4950–4959.
43. **Mosammaparast, N., and L. F. Pemberton.** 2004. Karyopherins: from nuclear-transport mediators to nuclear-function regulators. Trends Cell Biol. **14:**547–556.
44. **Munger, J., and B. Roizman.** 2001. The U(S)3 protein kinase of herpes simplex virus 1 mediates the posttranslational modification of BAD and prevents BAD-induced programmed cell death in the absence of other viral proteins. Proc. Natl. Acad. Sci. USA **98:**10410–10415.
45. **Ng, T. I., L. Keenan, P. R. Kinchington, and C. Grose.** 1994. Phosphorylation of varicella-zoster virus open reading frame (ORF) 62 regulatory product by viral ORF 47-associated protein kinase. J. Virol. **68:**1350–1359.
46. **Ogg, P. D., P. J. McDonell, B. J. Ryckman, C. M. Knudson, and R. J. Roller.** 2004. The HSV-1 Us3 protein kinase is sufficient to block apoptosis induced by overexpression of a variety of Bcl-2 family members. Virology **319:**212–224.
47. **Peng, H., H. Y. He, J. Hay, and W. T. Ruyechan.** 2003. Interaction between the varicella zoster virus IE62 major transactivator and cellular transcription factor Sp1. J. Biol. Chem. **278:**38068–38075.
48. **Perera, L. P., J. D. Mosca, W. T. Ruyechan, G. S. Hayward, S. E. Straus, and J. Hay.** 1993. A major transactivator of varicella-zoster virus, the immediate-early protein IE62, contains a potent N-terminal activation domain. J. Virol. **67:**4474–4483.
49. **Perera, L. P., J. D. Mosca, M. Sadeghi-Zadeh, W. T. Ruyechan, and J. Hay.** 1992. The varicella-zoster virus immediate early protein, IE62, can positively regulate its cognate promoter. Virology **191:**346–354.
50. **Piroozmand, A., A. H. Koyama, Y. Shimada, M. Fujita, T. Arakawa, and A. Adachi.** 2004. Role of Us3 gene of herpes simplex virus type 1 for resistance to interferon. Int. J. Mol. Med. **14:**641–645.
51. **Quensel, C., B. Friedrich, T. Sommer, E. Hartmann, and M. Kohler.** 2004. In vivo analysis of importin alpha proteins reveals cellular proliferation inhibition and substrate specificity. Mol. Cell. Biol. **24:**10246–10255.
52. **Rahaus, M., N. Desloges, M. Yang, W. T. Ruyechan, and M. H. Wolff.** 2003. Transcription factor USF, expressed during the entire phase of varicella-zoster virus infection, interacts physically with the major viral transactivator IE62 and plays a significant role in virus replication. J. Gen. Virol. **84:**2957–2967.
53. **Rihs, H. P., D. A. Jans, H. Fan, and R. Peters.** 1991. The rate of nuclear cytoplasmic protein transport is determined by the casein kinase II site flanking the nuclear localization sequence of the SV40 T-antigen. EMBO J. **10:**633–639.
54. **Ruyechan, W., P. Ling, P. Kinchington, and J. Hay.** 1991. The correlation between varicella zoster virus transcription and the sequence of the viral genome, p. 301–318. *In* E. K. Wagner (ed.), Herpesvirus transcription and its regulation. CRC Press, Boca Raton, Fla.
55. **Schaap, A., J. F. Fortin, M. Sommer, L. Zerboni, S. Stamatis, C. C. Ku, G. P. Nolan, and A. M. Arvin.** 2005. T-cell tropism and the role of ORF66 protein in pathogenesis of varicella-zoster virus infection. J. Virol. **79:**12921–12933.
56. **Schumacher, D., B. K. Tischer, S. Trapp, and N. Osterrieder.** 2005. The protein encoded by the US3 orthologue of Marek's disease virus is required

for efficient de-envelopment of perinuclear virions and involved in actin stress fiber breakdown. J. Virol. **79:**3987–3997.

57. **Soong, W., J. C. Schultz, A. C. Parera, M. H. Sommer, and J. I. Cohen.** 2000. Infection of human T lymphocytes with varicella-zoster virus: an analysis with viral mutants and clinical isolates. J. Virol. **74:**1864–1870.
58. **Spengler, M. L., W. T. Ruyechan, and J. Hay.** 2000. Physical interaction between two varicella zoster virus gene regulatory proteins, IE4 and IE62. Virology **272:**375–381.
59. **Stevenson, D., K. L. Colman, and A. J. Davison.** 1994. Delineation of a sequence required for nuclear localization of the protein encoded by varicella-zoster virus gene 61. J. Gen. Virol. **75:**3229–3233.
60. **Tagawa, T., T. Kuroki, P. K. Vogt, and K. Chida.** 1995. The cell cycle-dependent nuclear import of v-Jun is regulated by phosphorylation of a serine adjacent to the nuclear localization signal. J. Biol. Chem. **130:**255–263.
61. **Van Minnebruggen, G., H. W. Favoreel, L. Jacobs, and H. J. Nauwynek.** 2003. Pseudorabies virus US3 protein kinase mediates actin stress fiber breakdown. J. Virol. **77:**9074–9080.
62. **Xia, K., N. A. DeLuca, and D. M. Knipe.** 1996. Analysis of phosphorylation sites of herpes simplex virus type 1 ICP4. J. Virol. **70:**1061–1071.
63. **Xia, K., D. M. Knipe, and N. A. DeLuca.** 1996. Role of protein kinase A and the serine-rich region of herpes simplex virus type 1 ICP4 in viral replication. J. Virol. **70:**1050–1060.
64. **Zabierowski, S., and N. A. DeLuca.** 2004. Differential cellular requirements for activation of herpes simplex virus type 1 early (tk) and late (gC) promoters by ICP4. J. Virol. **78:**6162–6170.
65. **Zhang, F., R. L. White, and K. L. Neufeld.** 2000. Phosphorylation near nuclear localization signal regulates nuclear import of adenomatous polyposis coli protein. Proc. Natl. Acad. Sci. USA **97:**12577–12582.